Transport and Turbulence Studies in the T-10 Tokamak

T-10 Team (presented by M. V. Ossipenko)

Nuclear Fusion Institute, RRC "Kurchatov Institute", Moscow, Russia
e-mail: marina@nfi.kiae.ru

Abstract. Transitions to the improved confinement regimes were studied in the T-10 ECR heated tokamak: the H-mode with and without ITB and the pellet enhanced confinement (PEC) regime. It was shown that subtle changes in the q profile allow us to obtain either ITB or ETB only, or both of them under approximately similar conditions. The H-mode is obtained by power increase, pellet injection and biasing. The confinement time in the PEC-mode is 30% higher than that in the spontaneous H-mode. In biasing experiments the enhancement factor for the energy confinement time was up to 1.55. The global confinement in the regime with density above the Greenwald limit under strong gas puffing and ECRH was investigated. To identify the type of turbulence responsible for transport, Ohmic and ECRH regimes with variation of q_L and gas puffing were considered. Two regions along the minor radius with different turbulence properties corresponding to ITG or DTEM and resistive interchange instabilities were observed.

1. Introduction

This paper reviews the recent progress in understanding of the fundamental mechanisms of heat and particle transport in the improved confinement regimes in the T-10 tokamak. The distinctive feature of T-10 operation is the pure electron heating, which allows us to verify the theoretical predictions, validated in other tokamaks with predominantly ion heating, in conditions with hot electrons. In spite of the great progress in obtaining the improved confinement regimes, the fundamental mechanism of tokamak transport has not yet been identified. The following questions should be resolved: what is the physical mechanism of "profile consistency"? Is the "profile consistency" violated in the regimes with transport barriers? Under what conditions does the "critical gradient" model work? Is the instability responsible for the transport, global or local, and how does it determine the global scaling for the energy confinement time? If it is global, how is it related with the rational magnetic surfaces and TB formation? If it is local, is it possible to identify the microturbulence mode (ITG, ETG, DTEM)?

Having in mind these questions, experimental research in T-10 was developed in the following directions: studies of the heat and particle confinement in discharges with high density close to the limit value; consideration of changes in temperature and density profiles and transport coefficients due to the ECRH switch on/off; definition of the necessary conditions for ITB formation; H-mode transition by means of ECRH power increase, pellet injection and biasing; identification of the underlying mechanism of turbulence in Ohmic and ECRH plasmas.

2. Global Confinement Properties and Density Limit

A detailed comparison of the energy confinement time τ_E in T-10 with the intermachine scaling [1, 2] is presented in *FIG. 1* [3]. To separate the dependencies on plasma current I, plasma density n and input power P, the experimentally measured energy confinement time τ_E is normalized by $I^{0.9}B_T^{0.15}n^{0.4}P^{-0.7}R^2\varepsilon^{0.4}\cdot$ except the parameter under consideration in *FIG. 1* a)-c). The exponents, which were taken from the L-mode scaling [2]:

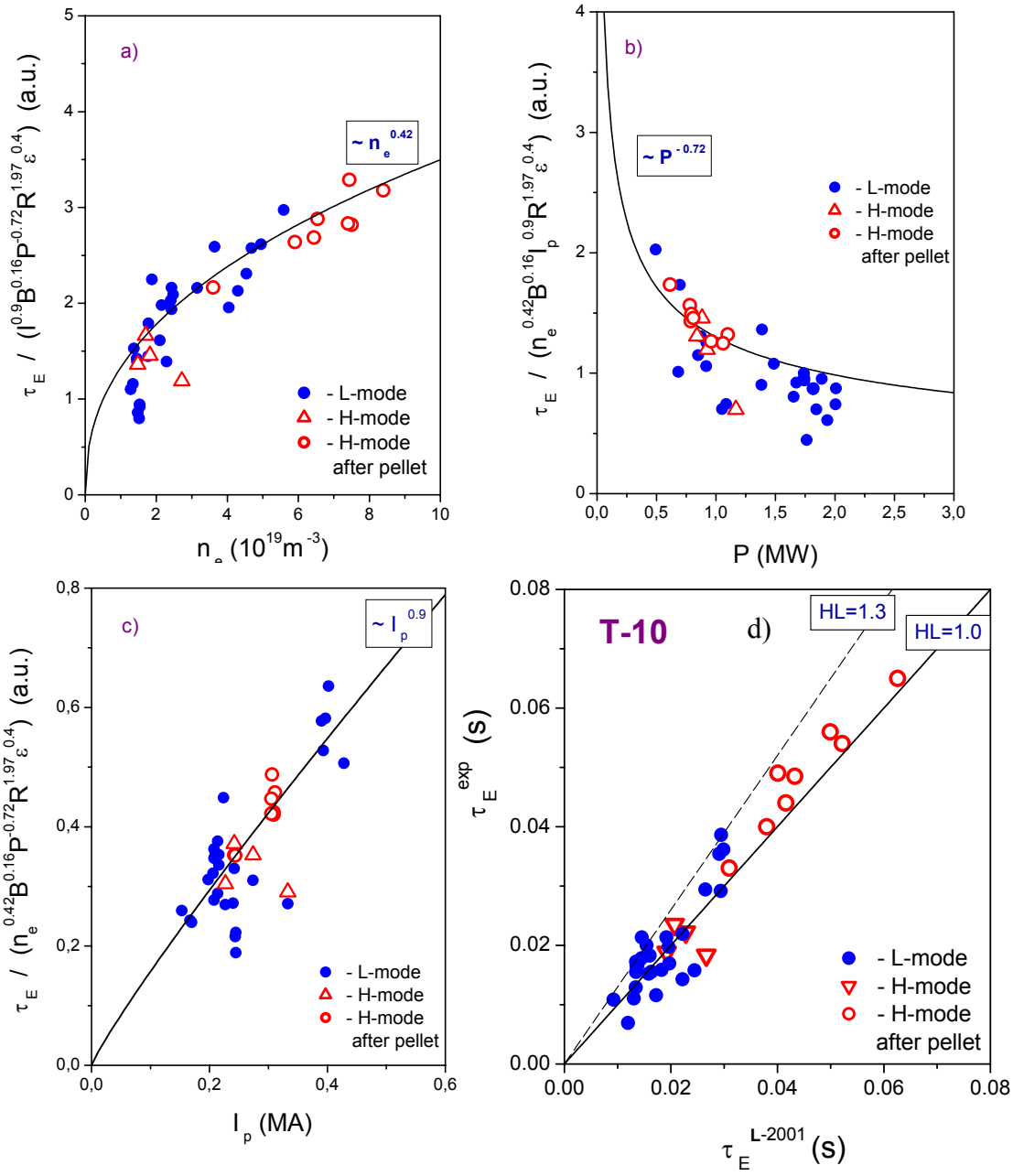

FIG. 1. Energy confinement time dependence on a) density, b) input power and c) plasma current. d) Comparison with the ITER scaling.

$$\tau_E^{L\text{-}2001}=0.026\, I^{0.81}B_T^{0.17}n^{0.43}P^{-0.75}R^{1.96}\varepsilon^{0.30}k^{0.86}M^{0.20}, \qquad (1)$$

describe the experimental trends well. It is important to note that the energy confinement in a tokamak with small size and pure electron heating shows main dependencies on plasma parameters consistent with the intermachine predictions obtained from the database for large tokamaks with predominantly ion heating. The peculiarity is that L and H mode scalings give very close values of τ_E for T-10, see *FIG. 1* d). The reason is that the statistically inferred scalings for τ_E^H and τ_E^L have very similar exponents:

$$\tau_E^{H\text{-}98(y,2)}=0.0562\, I^{0.93}B_T^{0.15}n^{0.41}P^{-0.69}R^{1.97}\varepsilon^{0.58}k^{0.78}M^{0.19} \qquad (2)$$

and, within the accuracy of exponents ± 0.1-0.15, their ratio depends on aspect ratio only

$$\tau_E^H/\tau_E^L = 2.16\, I^{0.12}B_T^{-0.02}n^{-0.02}P^{0.06}R^{0.01}\varepsilon^{0.28}k^{-0.08}M^{-0.01}\approx 2.16\, I^{0.12}\varepsilon^{0.28}. \qquad (3)$$

The first consequence of (3) is that in the core region *(ε<0.2)* the confinement in the L and H modes is indistinguishable and confinement improvement in the H-mode is determined by only the outer region *ε>0.2*. The second consequence is that for a tokamak with large aspect ratio (*ε=0.2* for T-10) the confinement improvement in the H mode can not be substantial.

The increase of the energy confinement time with the density according to scaling (1) seems to enable us to reach high confinement, when the density is close to the limit value n_{lim}. The limit is mainly determined by the MHD activity of the *m=2* mode, which is destabilized by the cooling of the plasma periphery. In T-10 ECRH discharges with strong gas puffing, the experimentally measured density limit was compared with the density limit estimated according to the Greenwald formula [4]:

$n_{lim} \approx n_{Gw}[10^{20}\ m^{-3}] = I[MA]/(\pi a^2\ [m^2])$. (4)

It was shown that the experimentally measured n_{lim} considerably exceeds n_{Gw} (by a factor of 1.8) in the discharges with high safety factor $q_L \approx 10$, but the ratio n_{lim}/n_{Gw} decreases with the plasma current increase, *FIG.* 2 a). This effect is due to the current profile shrinking with q_L rise. If the Greenwald formula (4) is modified by the replacement of the limiter radius by the current radius a_c, the ratio n_{lim}/n_{Gw} does not depend on the plasma current. In the calculations presented in *FIG.* 2 a), a_c is defined as the radius of the magnetic surface enclosing 95% of the plasma current. So n_{lim} does not exceed the modified Greenwald density limit.

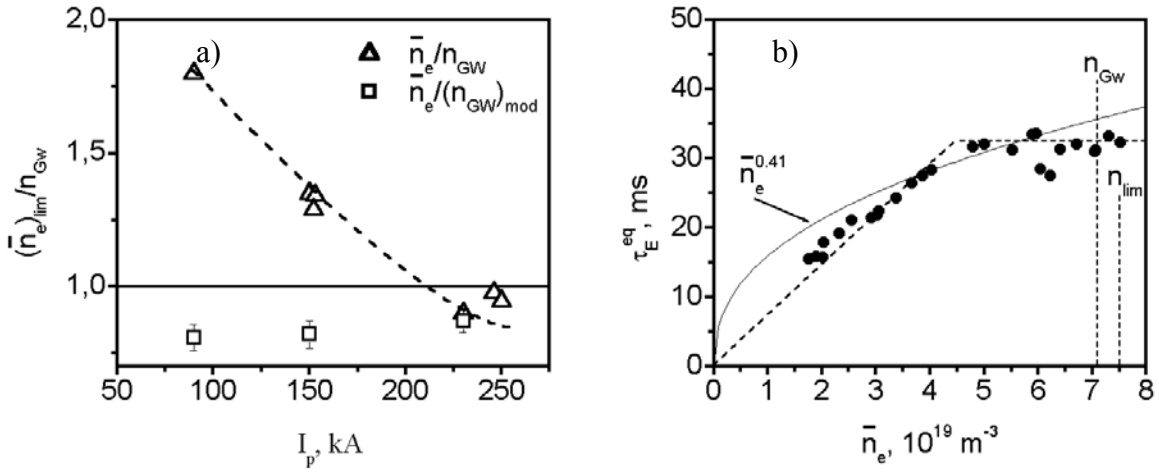

FIG. 2. a) Δ: dependence of the ratio n_{lim}/n_{Gw} on plasma current I_p, □: the same dependence for modified Greenwald limit n_{lim}/n_{Gw}^{mod}, b) $\tau_E/\tau_E^{96\text{-}L}$ dependence on density.

The dependence of τ_E on density was studied in the range $\bar{n}=0.2\text{-}1.1n_{Gw}$ *(I_p=200 kA, B=2.5 T)*. As is shown in *FIG.* 2 b), τ_E has a linear dependence on density while $\bar{n}<0.6n_{lim}$ and then saturates for the discharges with quasi-stationary density [5]. The saturated value of τ_E exceeds by *20%* the value given by the L-mode scaling ITER 96-L and it is close to the value predicted by the H-mode scaling ITER 98H(y,2). So the global confinement does not deteriorate substantially in the high density ($\approx n_{Gw}$) regime under gas puffing and ECRH. The saturation of τ_E seems to be due to development of electron rather than ion turbulence.

3. Studies of the Electron Heat Transport

From the very beginning of ECRH experiments on T-10, "the stiffness" or "consistency" of the electron temperature profile with respect to the external perturbation was observed and investigated [6]. The first formulation of the "profile consistency principle", that is self-organization of the plasma heat transport to produce the "canonical" temperature profile, was done by B. Coppi and then developed by B.B. Kadomtsev.

An excellent localization of the ECRH power (the half-width of the power absorption profile is less than 10% of the minor radius) allows us to verify the "profile consistency principle". *FIG.* 3 illustrates the "profile consistency" in a recent series of experiments with on- and off-axis ECR heating. Two shots with approximately the same total power are compared: #32915 (100% on-axis power) and #32918 (30% on-axis power and 70% off-axis power). Although the specific power on the axis was lower by a factor of 3 in the second shot, the electron temperature profiles differ by less than 10 % in these shots. Because the values of

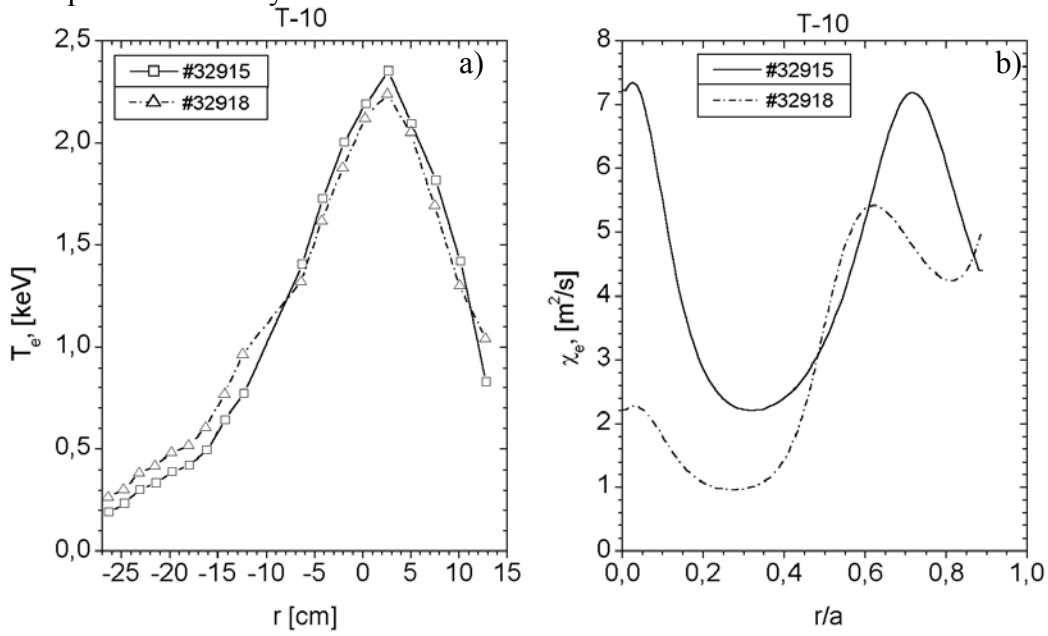

FIG. 3. Comparison of the temperature profiles (a) and the heat diffusivities (b) for the peaked (□ – solid line) and flat (Δ – dashed line) profiles of the ECRH power deposition.

temperature and density and their gradients are very similar for shots with on- and off- axis heating and the ratio of thermal diffusivities χ^{on}/χ^{off} is about *3* (for *r/a<0.4*), the question arises of what is the "hidden" variable responsible for the difference of transport for similar profiles.

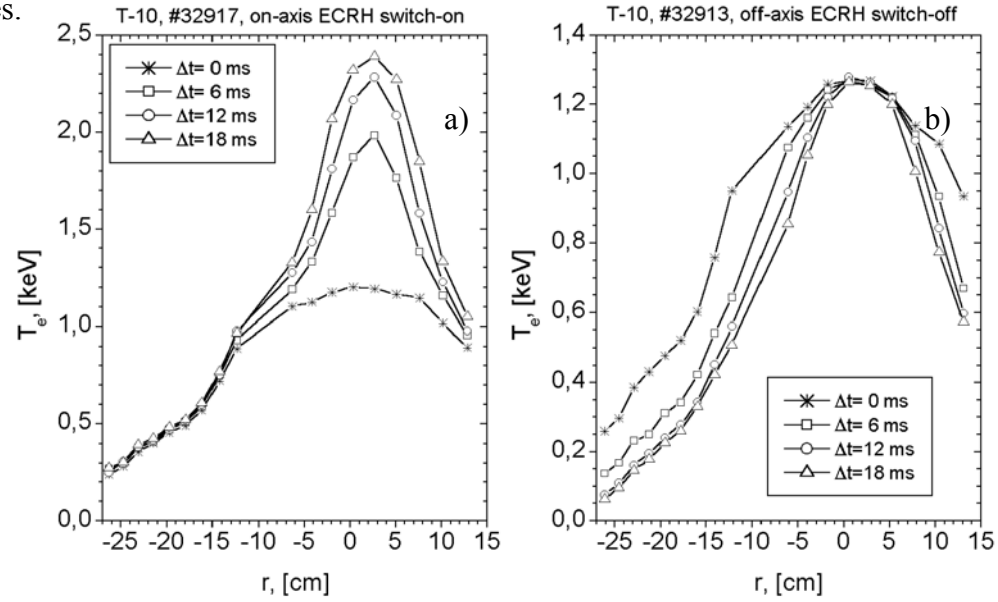

FIG. 4. ECE T_e profile evolution for a) on-axis ECRH switch-on, b) off-axis ECRH switch-off.

The changes in the heat fluxes due to on-(off-)axis ECRH switch-on (-off) were investigated in T-10 in a series of discharges #32905-#32921 with low density $\bar{n}=1.4\cdot10^{19}m^{-3}$. First, the sawtooth activity was suppressed by the off-axis ECRH (two gyrotrons, 140 MHz) at $\rho=r/a\approx0.4$, and then the third gyrotron was switched on at the same place, $\rho\approx0.4$, or at the center $\rho\approx0$. Two interesting effects were found: 1) the localized (inside $r=14$ *cm*) temperature rise after the on-axis ECRH was switched on against a background of two off-axis gyrotrons, *FIG.* 4 a); 2) the time delay (*20-40 ms*) between the ECRH power switch-off and the temperature drop at $r<4$ *cm*, *FIG.* 4 b).

The changes of the transport coefficients due to ECRH switch-on(-off) were analyzed by the numerical code COBRA based on the inverse problem solution for the reconstruction of the diffusive and convective parts of the heat flux during the transient processes. It is shown that invoking the "jumps" (changes with time less than 0.1ms) in transport coefficients allows us to describe the experimentally observed time traces of the electron temperature [7]. *FIG.* 5 shows the comparison of the experimental and calculated T_e increment after the on-axis ECRH switch-on against a background of two off-axis gyrotrons. It was found that the effective heat diffusivity has a minimum at the region of steepest gradient (which corresponds to $q\approx1$). ECE channels in this region show a linear (rather than exponential) T_e rise. So, this zone could be considered as the transport barrier, if only we did not know that at the stationary phase the T_e profile appears to be very close to the usual one for on-axis ECRH, *FIG. 3*. This means that all peculiarities are due to preliminary off-axis ECRH.

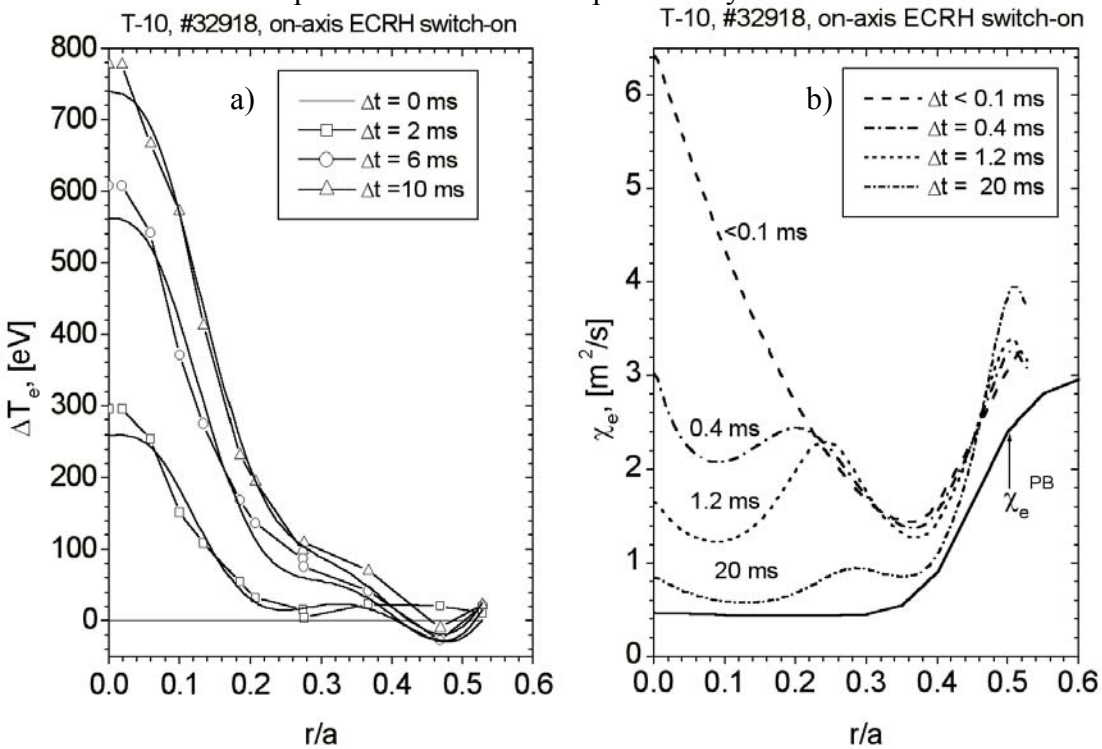

FIG. 5. a) T_e increment after the on-axis ECRH switch-on; b) χ_e "jump".

To analyze heat transport changes due to off-axis ECRH separately, let us consider discharge #32913, *FIG.* 6. The power balance (PB) analysis shows extremely low electron heat diffusivity $\chi_e^{PB}\approx0.2\ m^2/s$ (a factor of two below the Ohmic level) inside the radius of the off-axis ECRH power deposition ($t=550$-620 *ms*). Note that the characteristic normalized gradient $R/L_T\equiv(R/T_e)(dT_e/dr)$ is also a factor of two less than in the Ohmic regime (because the value of T_e increased but the gradient was not changed). At the front of the inward cold pulse propagation (CPP) due to switch-off of the off-axis ECRH ($t=620$ *ms*), R/L_T increases up to

17 compared with *10* in the Ohmic regime. But the dynamic value of χ^{CPP}, taken from the numerical analyses of the CPP, is *≈0.1,* which is close to the PB value at the end of the CPP. Typically in the Ohmic regime, $\chi^{CPP} \approx 1\ m^2/s$. That is, inside the radius of the off-axis ECRH power deposition, the improved confinement region appears ($\chi^{CPP} \approx 0.1\ m^2/s$, for $r/a<0.4$) with the χ values typical for the ITB region.

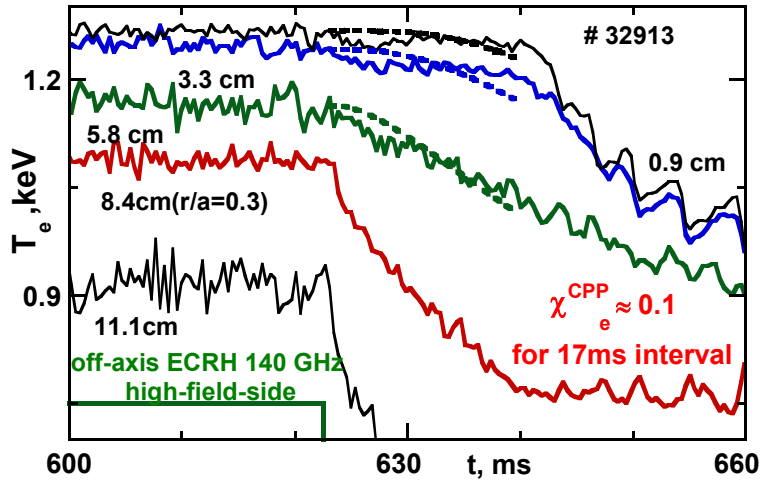

FIG. 6. ECE T_e evolution for the inward CPP due to off-axis ECRH switch-off (solid line - experiment, dashed line - modelling).

The presence of improved confinement zone in the off-axis ECR heated plasma has been confirmed when an additional on-axis ECRH (*0.55 MW*) was applied. Outward heat pulse propagation (HPP) showed $\chi_e^{HPP} \approx 0.2 - 0.3\ m^2/s$ in the zone $0.2< r/a < 0.37$, while the R/L_{Te} reaches *23* on the heat wave front, it is more than twice as high as the Ohmic value. Numerical analysis of the HPP created by smaller (*~0.06 MW*) on-axis ECRH shows similar values of χ_e^{HPP} and confirms the validity of the analysis for *0.55 MW* heating. This effect was first mentioned in [8].

One should note that there is a similarity of temperature profiles in Ohmic and on-axis ECRH regimes. For example, in shot #32913, $T_e^{EC}/\ T_e^{OH}=2\text{-}2.13$, that is, these profiles must be close to the "canonical" one (R/L_T is the same in ECRH and OH regime). But in the case of off-axis ECRH, $T_e^{EC}/\ T_e^{OH}$ changes from *1.15* at the center to *1.7* at the edge and the profile is below the "canonical" one determined by the current profile. So one can suppose that the heat diffusivity is low while the temperature profile is below the "canonical" one (R/L_T is below the critical value). Low transport in the core allows us to achieve improved confinement if the on-axis power deposition does not initiate substantial current redistribution.

The necessary condition for the confinement improvement is the ECRH power deposition beyond the *q=1* surface. In this case, off-axis ECRH can lead to current redistribution around the *q=1* surface to provide a zone of weak magnetic shear, which is favorable for barrier formation. This condition had been validated by the variation of the mutual position of *q=1* and of the power deposition by means of plasma current changes or by the variation of the toroidal magnetic field [9]. The central temperature increment due to on-axis ECRH switch-on against a background of off-axis ECRH was substantially higher when the off-axis power was deposited outside *q=1*. After the off-axis ECRH switch-on at *t=550 ms* (#32913), the sawtooth activity disappeared in *≈20 ms*. The gradual decrease of the phase inversion radius on the ECE T_e profile shows that the *q<1* region disappeared due to current redistribution. The current profile evolution was calculated by the ASTRA code with the experimental

profiles of T_e, n and Z_{eff}. The current was forced out of the plasma center due to the temperature profile broadening together with Z_{eff} peaking. The time of appearance and disappearance for the sawtooth oscillations in experiment and the corresponding time for the *q=1* surface in calculations are coincident. So the current changes together with the corresponding *q* profile modification can be responsible for the effect of extended confinement improvement (*20-40 ms*) in the core after the off-axis ECRH switch-off.

It was shown that subtle changes in q profile allow us to obtain either ITB or ETB only, or both of them under approximately similar conditions. Two very similar discharges with the *850 kW* off-axis ECRH (r_{ECRH}=*10cm*) and the *25%* current ramp-up are compared: #33041 (q_L=*3.9→3.04*, only the ITB is formed) and #33038 (*q=2.9→2.5*, only the ETB is formed), *FIG.* 7. In order to force the ITB to manifest itself, additional *450 kW* on-axis ECRH was applied. The core temperature rise is three times higher in #33041 than in #33038. Presumably this effect is due to the location of ECRH power input with respect to the *q=1* surface.

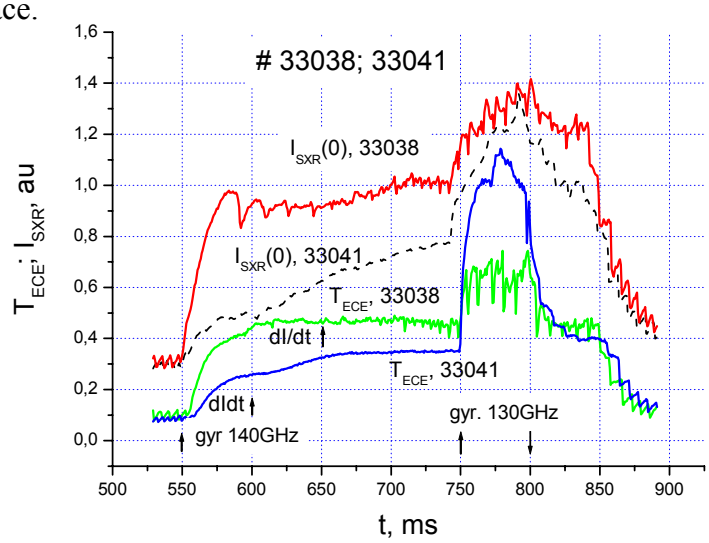

FIG. 7. Central ECE T_e and SXR signals evolution.

Comparison of the temperature profiles in *FIG.* 8 shows that the core confinement in #33041 is really improved compared with the usual central heating without the barrier, although global W and τ_E are higher in #33038, because the ETB exists in this discharge and provides better confinement due to wide profiles of temperature and density.

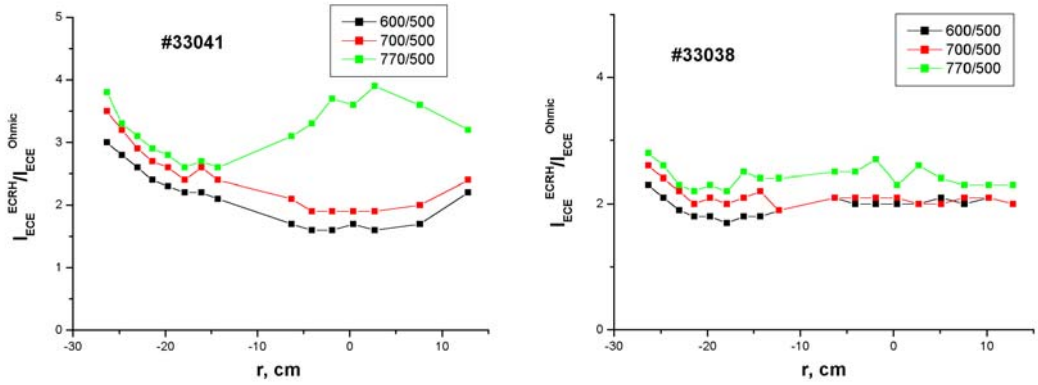

FIG. 8. The temperature profile normalized to the Ohmic one for discharges with ITB (#33041) and without ITB (# 33038).

4. H-mode Modelling

The H-mode regimes obtained in T-10 were analyzed with the four-field Edge Turbulent Layer model (ETL model) used as a boundary condition of the second kind for the ASTRA transport code. The model is able to simulate the ETB formation on density and temperature profiles near the rail limiter accompanied by the spontaneous increase of the stored energy and averaged density, and by D_α emission drop. The best fit to reproduce T-10 data was obtained under the assumption of the equality of parallel and perpendicular dissipation in turbulent structures. In this case the ETB width scales as $L \approx 2.1\rho^{2/3}R^{1/3}$ (ρ -ion Larmor radius) and is typically $L \approx 1 \div 2$ *cm*. The calculated sheared flow amplitude, necessary for turbulence suppression, is $V_p \approx 5000$ *m/s,* which agrees with the amplitude of the sheared electric field measured in the pedestal, $E_r \approx 100$ *V/m*. The turbulent heat and particle diffusivities are $D_{turb} \approx \chi_{turb} \approx 1\text{-}2$ m^2/s. The pedestal pressure gradient was found to be the control parameter which determines the L-H transition boundary. The analytical estimate for the value of the critical gradient $\nabla p_{L\text{-}H} \approx 3.89 \cdot n_{Le} \cdot T_{Le}/L$ (n_{Le}·and T_{Le} are taken at the radius of the rail limiter) was found from the ETL model. This estimate allows us to determine the L-H transition boundary on the T_{e_ped} - n_{e_ped} operating diagram. In *FIG. 9* the calculated points for the L-H transition and the analytical approximations are shown for DIII-D (open circles and solid line, $T_{e\_ped} \approx 0.03 + 0.1/n_{e\_ped}$) and T-10 (black circles $T_{e\_ped} \approx 0.1/n_{e\_ped}$).

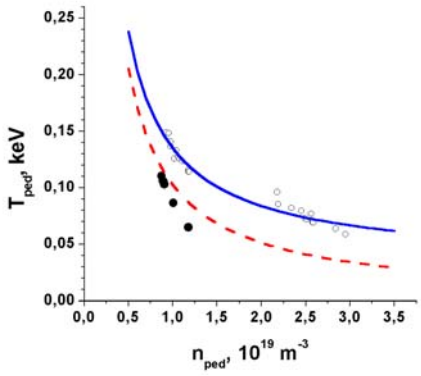

FIG. 9. L-H transition boundary for DIII-D (open circles) and T-10 (black circles).

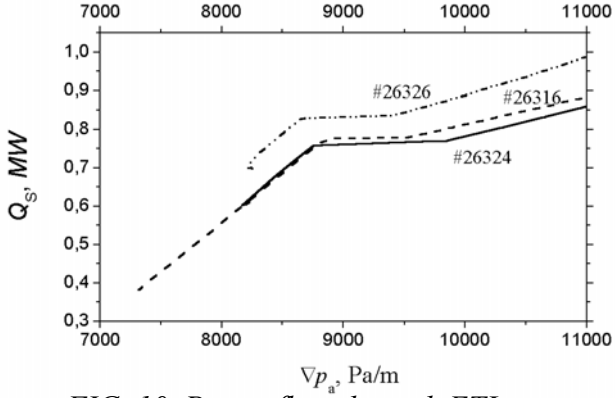

FIG. 10. Power flow through ETL vs pedestal pressure gradient.

The power threshold of the L-H transition is determined from the dependence of Q_S (the power flow through the ETL) on ∇p^{ped}, *FIG. 10*. The slope is proportional to the effective diffusivity in the L- and H-modes: $\chi_H / \chi_L \approx 1/3$. The L-H transition corresponds to the plateau on the plot; this value, $Q_S = Q_{L\text{-}H}$, is the power threshold for T-10: $Q_{L\text{-}H} = 0.75\text{-}0.85$ *MW*. The calculated power threshold dependence on density agrees well with the ITER scaling: $P_{th}^{ITER} = 1.66 \cdot \bar{n}_e^{0.58}$ **(**TABLE I**).** In T-10 the power threshold is almost independent of q.

TABLE I: L-H TRANSITION POWER DEPENDENCE ON DENSITY

#	$\bar{n}_e$, 10^{20} м$^{-3}$	Q_s, MW	P^{ITER}, MW
26308	**0.15**	**0.57**	**0.55**
26324	**0.225**	**0.69**	**0.7**
26326	**0.3**	**0.82**	**0.83**

The calculated confinement enhancement factor $H = \beta^H/\beta^L$ decreases with the increase of the q_L limiter and averaged density, *FIG.* 11, which corresponds to trends observed in T-10. Note that we compare β^H and β^L for the H and L phases of the same discharge. This means that the enhanced confinement can be mainly due to the density increase.

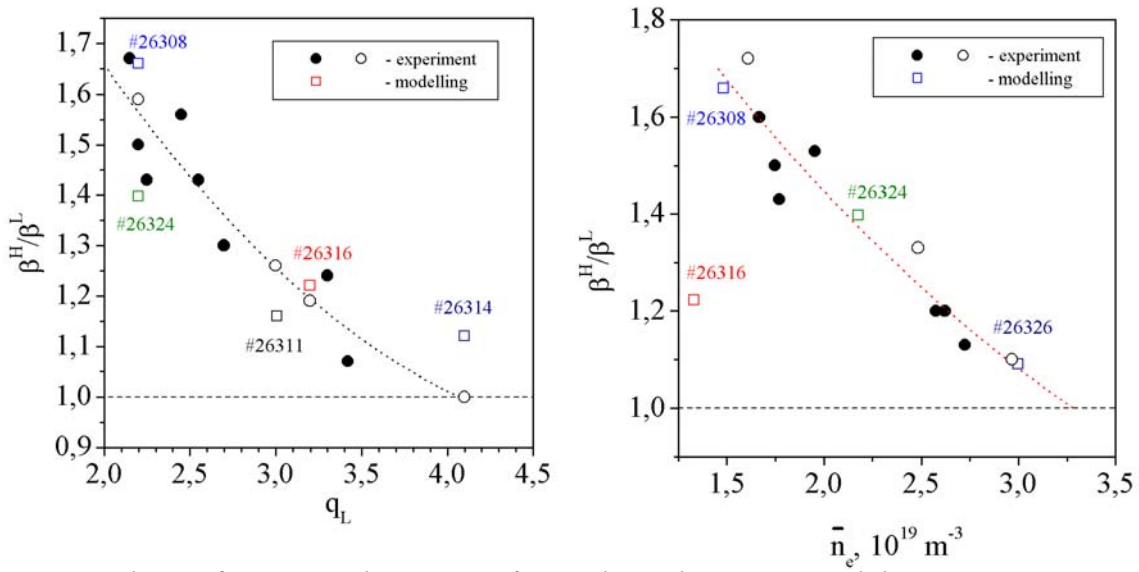

FIG. 11. The confinement enhancement factor dependence on q and density.

5. Biasing Experiments

The main goal of the biasing experiments was to study the radial electric field effect on turbulence reduction, on particle and heat confinement and on impurity exhaust [10]. Positive voltage (+450 V), applied to the electrode inserted 2 cm inside the rail limiter, results in the H-mode transition, while the ECRH power was below the threshold of the spontaneous L-H transition. The H-mode is identified by the D_α emission drop, the edge pressure gradient increase (inside the position of the electrode) and the energy confinement time increase.

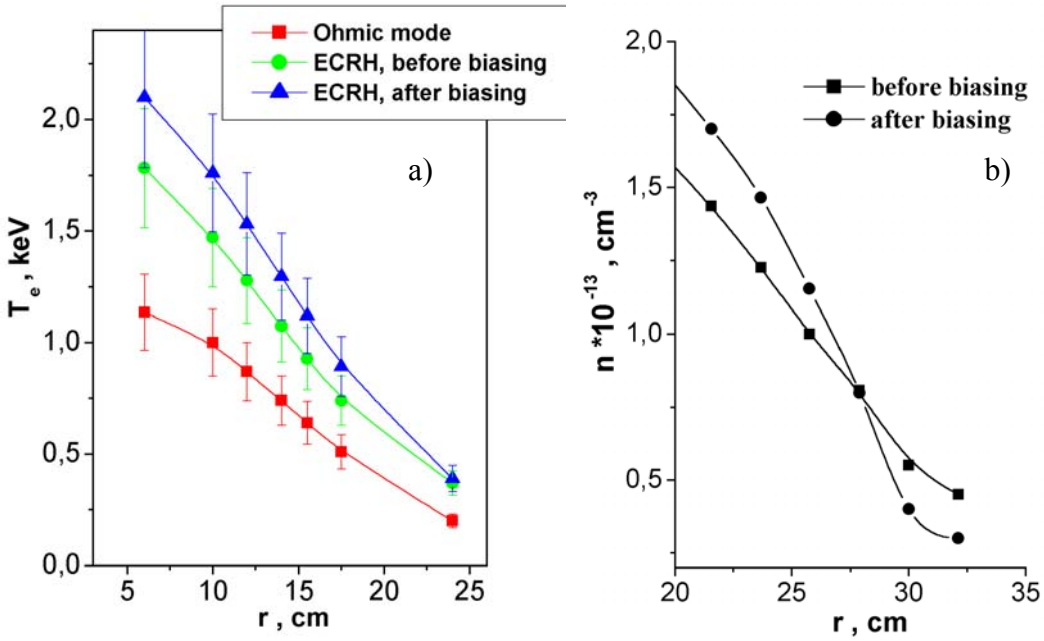

FIG. 12. Comparison of the temperature (a) and density (b) profiles before and after biasing.

The peculiarity of T-10 compared with other biasing experiments [10] is the *15%* T_e rise and *30%* T_i rise together with *30%* n rise after biasing, *FIG.* 12, while in other tokamaks only n rise was observed.

To determine whether τ_E increases owing to biasing or density rise, two discharges with different initial densities and other parameters similar are compared in *FIG.* 13. The discharge #29583 before biasing has the same density and inductance l_i as discharge #29580 after biasing, but the β is higher in the latter case. So the *30%* increase of τ_E is due to biasing in discharges with the same density. The confinement improvement with respect to the L-mode of the same discharge is even more considerable: $\tau_E^H/\tau_E^L \approx 1.5\text{-}2.6$. The ratio approaches unity for higher densities, $\tau_E^H/\tau_E^L \approx 1$ for $n > 3.5 \cdot 10^{19}$ m^{-3}. The enhancement factor for the energy confinement time with respect to ITERH-IPB98(y,2) can be up to 1.55 (*FIG.* 14).

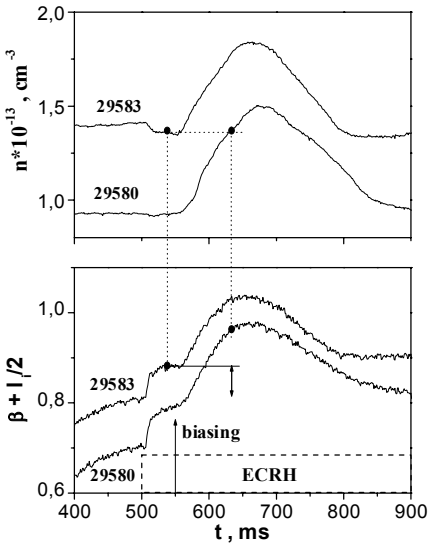

FIG. 13. Comparison of β in regimes with different density.

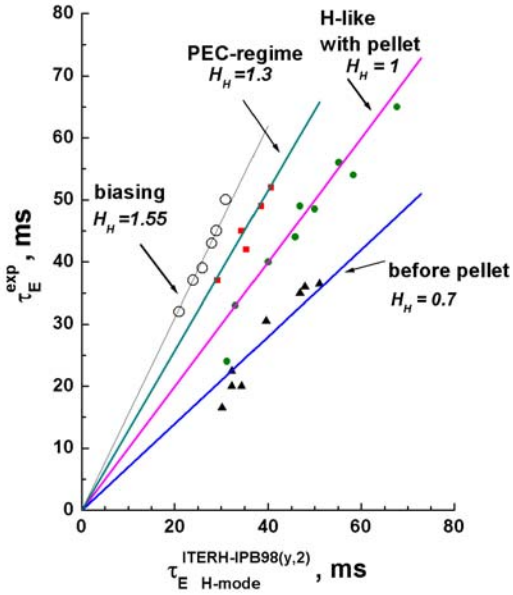

FIG. 14. Comparison of the H-mode τ_E with the ITER scaling.

6. Pellet Injection

The injection of D_2 pellets from the low toroidal field side into the ECRH plasma in T-10 leads to two regimes with improved confinement. In the PEC-mode after the pellet injection the averaged plasma density first grows and then falls to the initial level, but with a more peaked profile. In the H-like mode the density does not fall but remains constant during the whole ECRH pulse (in a wide range up to the Greenwald limit). The experimental energy confinement time agrees with the ITER scaling for ELMy H-mode, *FIG.* 14. The confinement time in the PEC-mode is 30% higher than that in H-mode.

7. Turbulence Studies

To identify the type of turbulence responsible for transport, systematic studies of turbulent spectra were done in Ohmic and ECR heated (0.9 MW) discharges with variation of q_L (with plasma currents 165, 220 and 310 kA) and densities 1.6 and $2.5 \cdot 10^{19} m^{-3}$ (by gas puffing) [11]. The turbulence was investigated by means of correlation reflectometry and Langmuir probes.

Along the minor radius two regions with different turbulence properties were observed. The first one covers the main transport region with high temperature between *q=1* and *2*. In this region the turbulent spectrum consists of the broadband (*0-400 kHz*), the low-frequency (*0-50 kHz*, "streamer"- like) and the quasi-coherent (*50-250 kHz*) components and oscillations at *20 – 30 kHz*, having properties of "zonal flows". The turbulence rotates like rigid body with a constant angular velocity equal to that of the *m=2* mode rotation over all plasma radii. The calculations of the growth rates show that this turbulence may be driven by ITG or DTEM instabilities. The edge turbulence in the second region is unstructured and weakly correlated,, it's poloidal velocity is low. These properties are consistent with the predictions of the ETL model based on resistive interchange instability. The transition radius between the two regions coincide with the sheared velocity layer. The radius decreases when the plasma current diminishes or the density rises via gas puffing. To identify the driving mechanism for different types of turbulence, the transition (due to gas puff cut off) from saturated (SOC) to improved (IOC) Ohmic confinement regimes is considered. The decrease of the mean core turbulence wavelength, impurities peaking and decrease of ion heat conductivity were observed. It was shown that in the IOC case (the lowest power flow and maximal density peaking) the asymmetric component of LFS turbulence disappears and the wavelength shortens by a factor of 2-2.5 *FIG.* 15. The maximum of the quasi-coherent fluctuations (≈100 kHz in the SOC regime only at the LFS) shifts to *≈200 kHz* in the IOC regime and appears both at the LFS and at the HFS. Significant variation of the turbulence characteristics were measured at the start of the central ECRH and after fast edge cooling by carbon flake. In all cases the change of the core turbulence were interpreted as interplay between ITG and DTEM instabilities.

FIG. 15. Changes of turbulence in saturated (SOC) and improved (IOC) Ohmic confinement regimes.

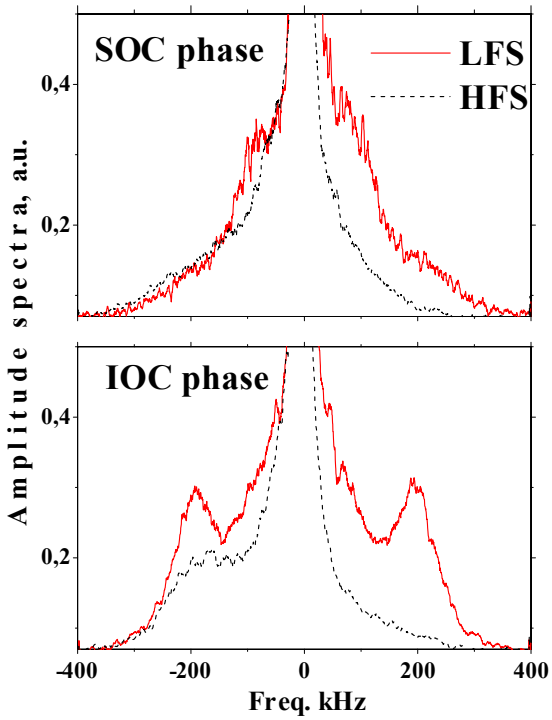

The first step to control the frequencies and amplitudes of the low m MHD modes by means of externally induced halo-currents was done in [12]. It could be a good tool to understand the links between the MHD modes and small scale turbulence. Direct measurements of the radial electric field and the corresponding **E×B** flow can be performed using a heavy ion beam probe.

8. Conclusions

It is shown that the statistically inferred intermachine ITER scaling for τ_E obtained for tokamaks with predominantly ion heating provides a good fit for parameter dependencies observed in T-10 with pure electron heating. So one can talk about a common physical mechanism which determines transport in a tokamak. Peculiarity of T-10 is the large aspect ratio; therefore τ_E predicted by the ITER scaling is almost the same for L and H regimes.

Transitions to the improved confinement regimes under ECRH were studied: the H-mode with and without ITB and the pellet enhanced confinement (PEC) regime. H-regimes obtained by ECRH power increase, by pellet injection and by biasing were modelled and compared. The most substantial improvement of both particle and energy confinement was observed in biasing experiments. In the PEC-mode the averaged plasma density was more peaked than in the H-mode with pellet. The confinement time in the PEC-mode is 30% higher than that in the H-mode. The observed positions of ITB and ETB are correlated with the position of the corresponding magnetic surfaces with low q. The subtle changes in q profile allow us to obtain either ITB or ETB only, or both of them under approximately similar conditions. This means that further investigation of the MHD modes' contribution to transport is necessary, because they seem to be responsible for the realization of the "canonical" profile.

"Jumps" of the transport coefficients due to ECRH switch on/off were discovered with the help of the numerical code COBRA. Both COBRA simulations and the heat pulse propagation analysis show that in the off-axis ECRH plasma there are domains with thermal diffusivities a few times lower than in the Ohmic discharges. Turbulent spectra analysis shows that the confinement improvement is connected with the transition from the ion (ITG) to the electron (DTEM) instability.

This work is supported by the Nuclear Science and Technology Department of Minatom RF, RFBR (Grant 00-15-96536) and INTAS (Grant 2001 - 2056).

References

[1] ITER Physics Basis, Chapter 2, Nucl. Fusion **39** (1999) 2175.
[2] BRACCO, G., "Energy Confinement Scaling in L-mode DB 2.7", ITPA Meeting of–Confinement Database and Modeling Group, 2001, Toki, Japan.
[3] LEONOV, V.M., CHUDNOVSKIY, A.N. "L- and H-mode confinement in T-10", ITPA Meeting of Confinement Database and Modeling Group, March, 2002, Princeton, USA.
[4] GREENWALD, M., et al., Nucl. Fusion **28**, 2199 (1988).
[5] KIRNEVA, N.A., et al., this conference, CD-ROM file EX/P3-01.
[6] ALIKAEV, V.V., et al., Nucl. Fusion **32** (1992) 1811.
[7] ANDREEV, V. F., et al., Plasma Phys. Reports **28** (2002) 367.
[8] BAGDASAROV, A. A., VASIN, N. L., NEUDACHIN, S. V., SAVRUKHIN, P. V. (Proc. 13th IAEA Conf. Washington, 1990) IAEA, Vienna (1991) V. 1, p. 253.
[9] RAZUMOVA, K.A. and T-10 Team, "Role of q(r) profile in the transport barriers formation on T-10 tokamak", this conference, CD-ROM file EX/P3-03.
[10] KIRNEV, G.S., et al., Czech. J. Phys. **51** (2001) 1011.
[11] VERSHKOV, V.A., et al., this conference, CD-ROM file EX/P3-04.
[12] IVANOV, N.V., et al, ibid., CD-ROM file EX/S2-3.